ORNL/TM-2022/2596

Large-Scale Additive Manufacturing of Silicon Carbide with Process Monitoring

M. Dylan Richardson
Austin T. Schumacher
Alexander M. Rogers
Christian M. Petrie

Approved for public release. Distribution is unlimited.

September 2022

M2CT-22OR1305012

OAK RIDGE National Laboratory

ORNL IS MANAGED BY UT-BATTELLE LLC FOR THE US DEPARTMENT OF ENERGY

ORNL/TM-2022/2596

Advanced Materials and Manufacturing Technologies Program

LARGE-SCALE ADDITIVE MANUFACTURING OF SILICON CARBIDE WITH PROCESS MONITORING

M. Dylan Richardson
Austin T. Schumacher
Alexander M. Rogers
Christian M. Petrie

September 2022

M2CT22OR1305012

Prepared by
OAK RIDGE NATIONAL LABORATORY
Oak Ridge, TN 37831
managed by
UT-BATTELLE LLC
for the
US DEPARTMENT OF ENERGY
under contract DE-AC05-00OR22725

CONTENTS

LIST OF FIGURES

LIST OF TABLES

ABBREVIATIONS

AM	additive manufacturing
AMMT	Advanced Materials and Manufacturing Technologies
ASME	American Society of Mechanical Engineers
AVS	Advanced Vacuum Systems
CAD	computer-aided design
CVI	chemical vapor infiltration
DOE-NE	US Department of Energy - Office of Nuclear Energy
FY	fiscal year
NQA-1	Nuclear Quality Assurance
ORNL	Oak Ridge National Laboratory
PVC	polyvinyl chloride
SiC	silicon carbide
TCR	Transformational Challenge Reactor

SUMMARY

This report summarizes new capabilities in additive manufacturing (AM) of large-scale silicon carbide (SiC) components under the Advanced Materials and Manufacturing Technologies (AMMT) program. SiC is a promising material that is being considered for many advanced reactor designs due to its high temperature strength, radiation tolerance, minimal neutron absorption, and oxidation resistance [1-8]. One of the primary limitations to using SiC as an in-core structural material is the inability to fabricate large SiC components with complex geometries. While under the former Transformational Challenge Reactor (TCR) program, ceramic AM systems at the Oak Ridge National Laboratory (ORNL) were limited in the quantity and overall size achievable for producing ceramic AM components. To address this, ORNL has improved its infrastructure for binder jet and chemical vapor infiltration (CVI) processes with cutting-edge equipment coming online in a newly renovated laboratory space capable of producing larger components and higher throughput without compromise on part size. This report details the laboratory renovation progress, focusing specifically on the DesktopMetal (formerly ExOne) X25Pro binder jet, a large scale CVI furnace, and the added functionality of a software tool called Peregrine for quality assurance and control purposes.

1. INTRODUCTION

The US Department of Energy Office of Nuclear Energy (DOE-NE) launched the TCR program with the goal of integrating additive manufacturing (AM) with modern modeling and simulation tools, in-situ process monitoring, and an agile approach to rapidly design, build, and operate a 3D printed advanced nuclear reactor core. The TCR program was successful in achieving the following:

- Demonstrating an agile design process to leverage AM and rapidly converge on an optimized, advanced nuclear microreactor design [9-15]
- Advancing new reactor materials such as an yttrium hydride moderator [16-22], AM 316 stainless steel (316SS) [23], AM silicon carbide (SiC) [24, 25], and the novel integration of uranium nitride tristructural-isotropic fuel [26] densely packed in an AM SiC matrix [27]
- Developing the digital platform necessary to certify and qualify AM materials for nuclear applications [28-30]
- Integrating and embedding spatially distributed sensors within AM materials for nuclear applications [31-34]
- Progressing toward semi-autonomous reactor operation [35, 36]
- Evaluating and understanding radiation effects on AM SiC [37, 38], 316SS [39], and integral TCR fuel compacts [27, 40]

In fiscal year (FY) 2021, the TCR program priorities shifted away from a nuclear reactor demonstration, but the focus on advancing ceramic AM for nuclear applications and qualifying AM components remained. Eventually, the TCR program was merged into the AMMT program and focused on the broader adoption of AM for nuclear applications compliant with American Society of Mechanical Engineers (ASME) Nuclear Quality Assurance (NQA-1) standards. Research activities are conducted on a quality "graded approach" whereby work activities apply increasing levels of quality and safety rigor according to the risk level of the specific task or product. This report summarizes work performed in FY22 to continue developing AM SiC for nuclear applications with a specific focus on transitioning to larger scale geometries while retaining the ability to monitor components during manufacturing to ensure proper quality control. Although this report focuses on AM process improvements for generic SiC components, the capabilities that have been established under this DOE-NE program are particularly relevant to multiple industry partners [41, 42] that have adopted nuclear fuel forms similar to the TCR concept.

Binder jet technology was selected for AM of SiC components because it is cost effective, capable of producing complex geometries, and is compatible with chemical vapor infiltration (CVI) required to densify the printed components. A previous report [43] provides details about the binder jet fabrication and densification processes. In previous efforts, size limitations on fabricating parts were caused by two main issues: (1) the Innovent+ binder jet system has a limited build volume of 160×65×65 mm, and (2) the CVI system used for densification is limited to a heating zone of approximately 152 mm in height and 76 mm in diameter. Because of these limitations, scaled up versions of the fabrication and densification processes are desired.

A DesktopMetal (formerly ExOne) X25Pro binder jet system was acquired to scale up the binder jet capabilities. This system enables a much larger build volume of 400×250×250 mm and improves upon the Innovent+ features, allowing for prints that can be left unattended for much longer periods of time and for fabrication of parts with greater initial (green) strength. In addition to these upgrades, a new camera system has been incorporated into the process to implement Peregrine [29] for monitoring prints in situ. Another added capability is the scaled up CVI furnace system acquired from Advanced Vacuum Systems (AVS). This allows for a larger heating zone with a volume of approximately 152×152×457 mm that will enable densification of the products made from the X25Pro system.

2. LABORATORY RENOVATIONS

Due to the larger footprint of the AVS CVI system, X25Pro, and X25Pro ancillary equipment, a lab space was repurposed to house them. As such, demolition and renovations were performed so the equipment could be installed. Figure 1–Figure 3 show the progress of the lab renovation in chronological order, from equipment initially being brought in to present. Many modifications were made to ensure a safe and useable lab space, including development of an active air monitoring system.

Figure 1. CVI equipment (left) and X25Pro (right) being installed.

Figure 2. Equipment when initially moved into the lab (left) and CVI system being installed (right).

Figure 3. Lab with lighting and equipment in place (left) and current progress on CVI system enclosure (right).

3. OVERVIEW OF BINDER JET PROCESS

The binder jet process involves several different steps that are independent of the system being used. First, a software code reads in a computer-aided design (CAD) model and slices it into sequential 2D layers based on the defined layer height. Before a print can begin, a foundational layer of powder must be deposited in several passes via the recoater, which drops and smooths powder across the print bed. Once the foundation layer is adequate, a printhead travels across the print bed, selectively depositing binder in the shape of the current layer. Further information on the general binder jet process can be found in previous reports and publications [24, 43].

3.1 X25PRO BINDER JET

The X25Pro binder jet system is similar to the M-Flex binder jet system produced by ExOne, with several notable improvements. The overall printable volume (400×250×250 mm) and the general printing process is the same. Figure 4 & Figure 5 show the X25Pro and its ancillary equipment. Unlike the Innovent+ system that was used for most of TCR, the X25Pro has two rollers—one which performs roughing, and one which performs smoothing. Utilizing this two-roller approach, powder spreading and compacting are both improved, allowing for the use of a wider variety of powders and a higher green density. An ultrasonic generator is used to dispense the SiC powder through a mesh screen like the Innovent+, and an auger is included in the recoater to keep the powder from getting stuck.

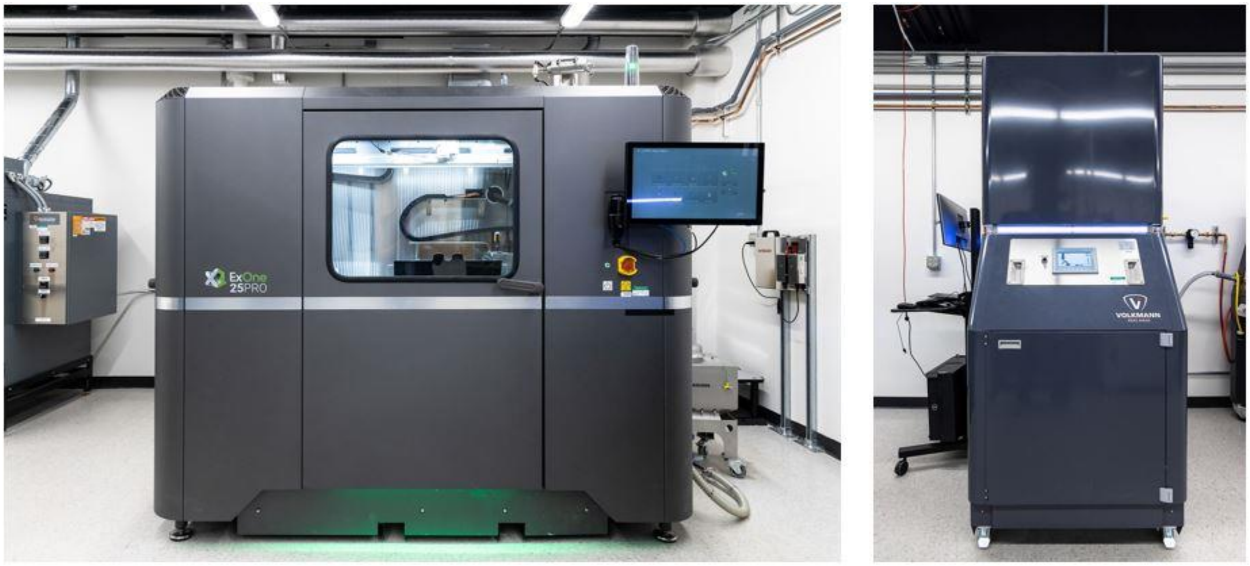

Figure 4. X25Pro (left) and powder recycler for sieving powder (right).

Figure 5. Curing oven and lift cart (left) and depowdering stand (right).

Because the X25Pro is much larger than the Innovent+, a different powder feed system is used to prevent the need to manually add powder during a print. The printer uses facility air to pull powder from a mobile hopper as needed. Sensors are in place to determine when additional powder is needed during a print. An overflow container catches excess powder, and the system can automatically pump in more cleaner and binder as necessary. These additions allow for prints to continue without operator intervention. The overflow container is connected to a powder recycler via polyvinyl chloride (PVC) tubing, and a conveyor system in the powder recycler transfers the powder for sieving. Powder can also be transferred from a job box after parts have been extracted in a similar manner. The mobile hopper is connected to the bottom of the powder recycler, where it collects any sieved powder.

With a few small additions to the lab space, a nearly closed system was designed to minimize contact with powder. Valves were added so that powder can be pulled from either the depowdering stand or the X25Pro without altering any connections or handling any tubing. Figure 6 shows a flow chart of the general process to fabricate parts with the X25Pro, and Figure 7 shows the plumbing added to minimize contact with powder.

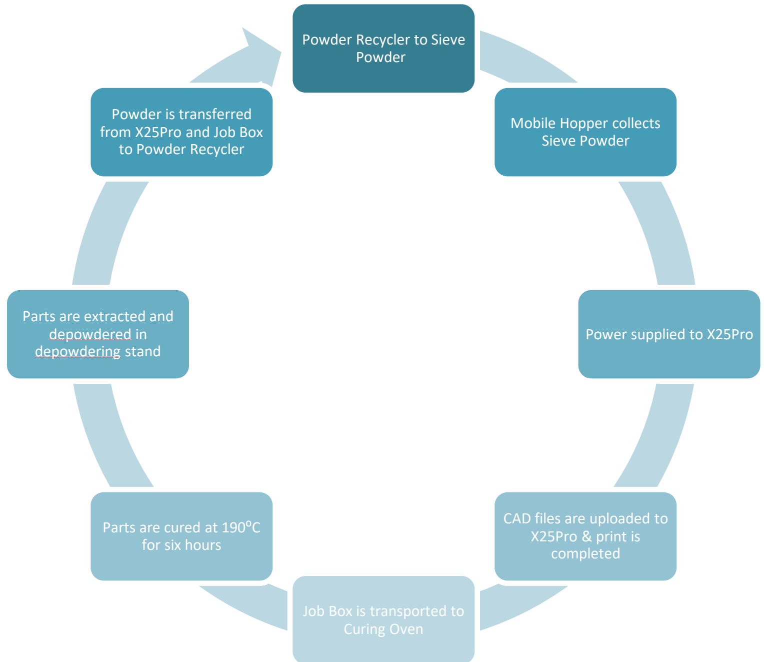

Figure 6. Flow chart of general steps for printing with the X25Pro.

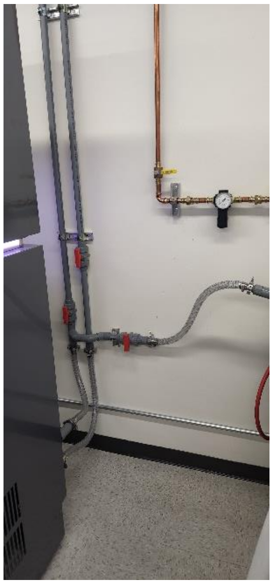

Figure 7. Powder transfer connections avoid the need to change connections.

3.2 PEREGRINE

Because AM of parts can have anomalies or defects on a layer-by-layer basis, parts can be difficult to qualify. For many industries (e.g., nuclear), this poses a problem, because very high levels of quality control and traceability are required. To mitigate this, a real-time detection and classification software was developed for pixel-wise localization of layer-wise imaging data. This software tool, Peregrine, enables advanced data analytics for powder bed AM and is compatible with several different powder bed AM processes (e.g., laser fusion, binder jet, and electron beam fusion) [29]. Peregrine has been successfully used with the Innovent+ for almost every SiC print under the TCR program, providing in-situ data for samples and components during fabrication. This allowed for swift explanations of observed defects or failures post fabrication. These monitoring technologies will be essential to support future digitally-informed certification of AM components.

The necessary cameras to utilize Peregrine during the printing process were mounted in the X25Pro. Unlike the Innovent+, which only uses a visible light camera, the X25Pro has both visible and infrared cameras. Because of the larger build area, the cameras require a larger field of view to capture the entire powder bed. The angle at which the cameras were mounted resulted in some distortion in captured images, but Peregrine effectively removes this distortion. Figure 8 shows the camera setup for the X25Pro, with a 3D printed case used to protect the cameras from any powder during a print. Figure 9 shows the raw image of a printed layer and the Peregrine images produced after analysis.

Figure 8. Job box with foundation layer of powder and cameras used for Peregrine mounted at the top.

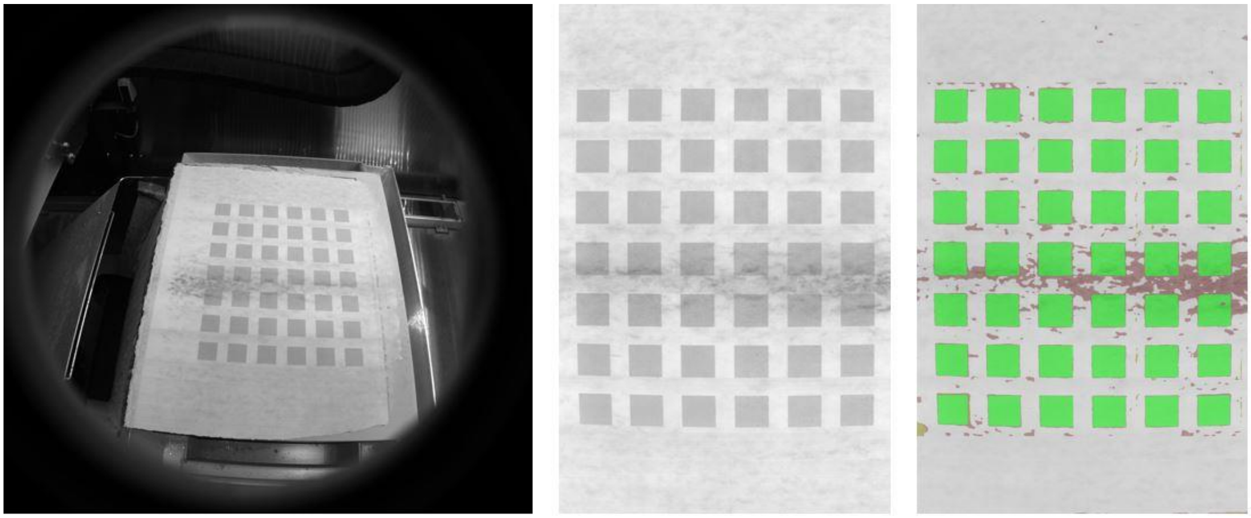

Figure 9. Raw camera image (left), distortion-corrected image (middle), and analyzed layer (right). The dark pattern was caused by the switch to a different lot of SiC powder. Green in the analyzed layers shows what Peregrine interpreted as the printed parts.

Although the initial X25Pro tests have not produced any prints with defects, Peregrine can detect and notify operators as any defects occur. Several examples from Innovent+ prints are shown in Figure 10–Figure 13. In Figure 10, one of the parts shifted early in the print, as detected by Peregrine. Figure 11 shows that same print several layers later, highlighting the fact that there is no evidence of the part shifting. Figure 12 shows an example of Peregrine detecting that there is inefficient binder for the parts, indicating an issue with the printhead's jets. Figure 13 shows an example of inefficient curing in which the roller causes binder to streak across the print bed.

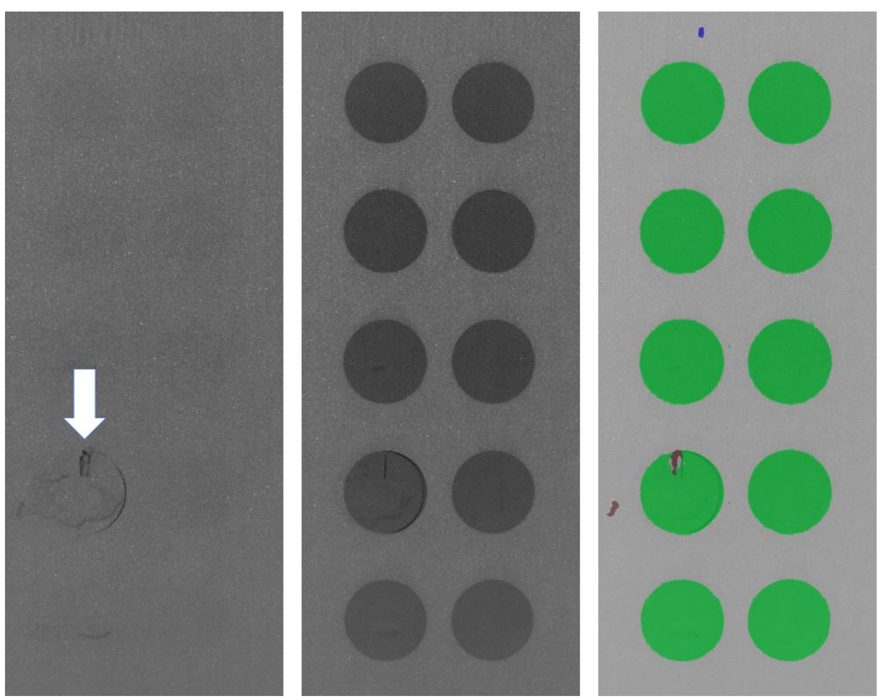

Figure 10. Example of Peregrine detecting a part shifting. The left image shows the powder bed, the middle image shows the shift after the binder was deposited, and the right image shows the analyzed layer from Peregrine.

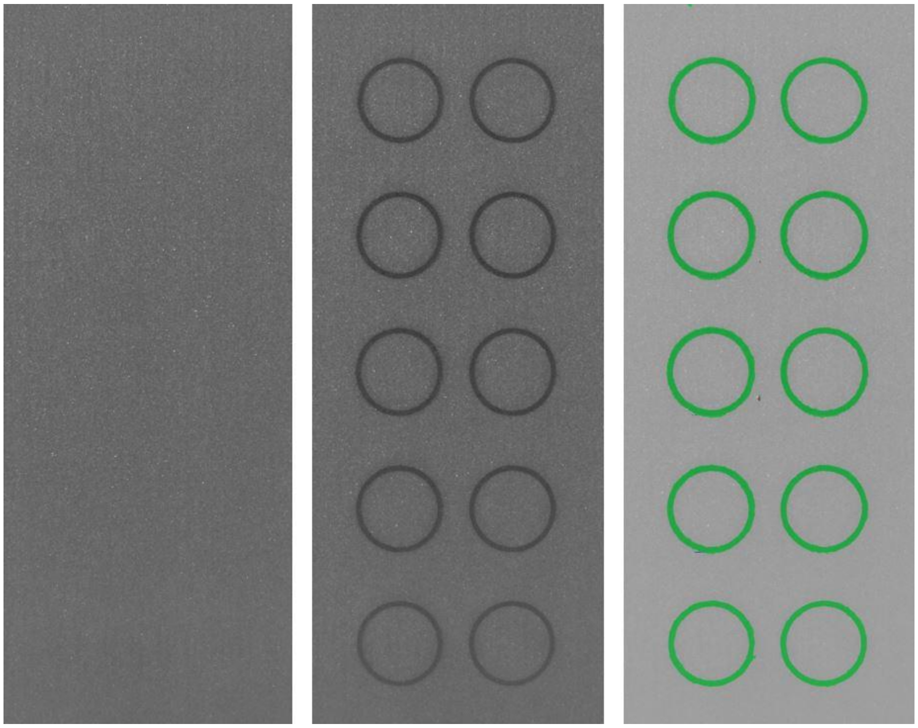

Figure 11. Images from several layers after the defect shown in Figure 12 showing no evidence of the compromised part.

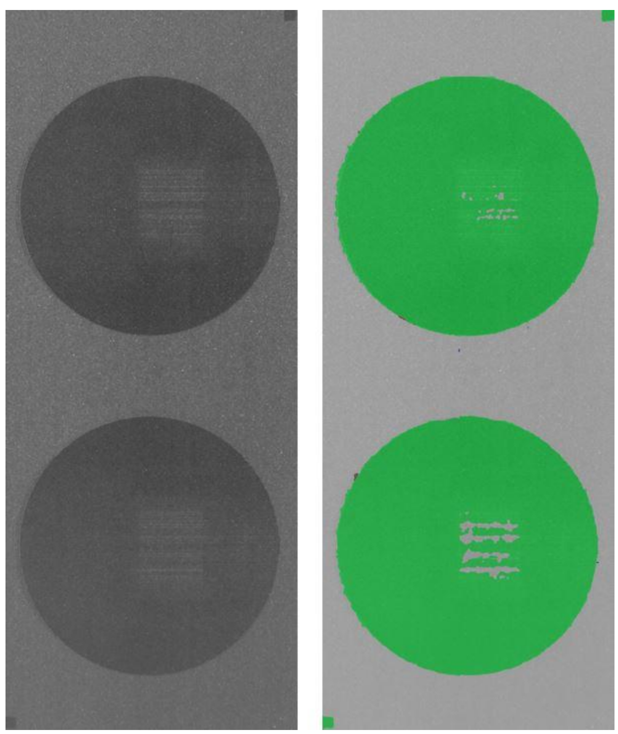

Figure 12. Example of Peregrine detecting inefficient binder dropping.

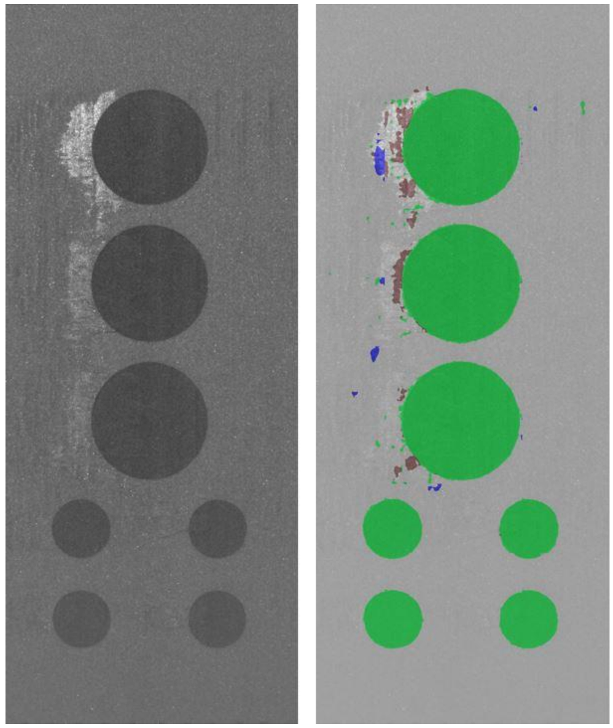

Figure 13. Example of inefficient curing, resulting in binder streaking.

4. INITIAL PRINTING RESULTS

For the initial print, a set of 25.4×25.4×5 mm cuboids were printed with a layer height of 50 µm. Two different powders were used, one provided by the vendor during the site acceptance test (SAT) and the other being the lot that was used under the TCR program. The former is micro grit F600 SiC and has an average particle size of approximately 10 µm. The latter is -400 mesh SiC from Sigma Aldrich and has an average particle size of approximately 20–30 µm, depending on the powder lot number. Figure 14 shows examples of cuboids printed using the vendor-provided SiC vs. the Sigma Aldrich SiC, displaying the clear differences in surface roughness and overall quality.

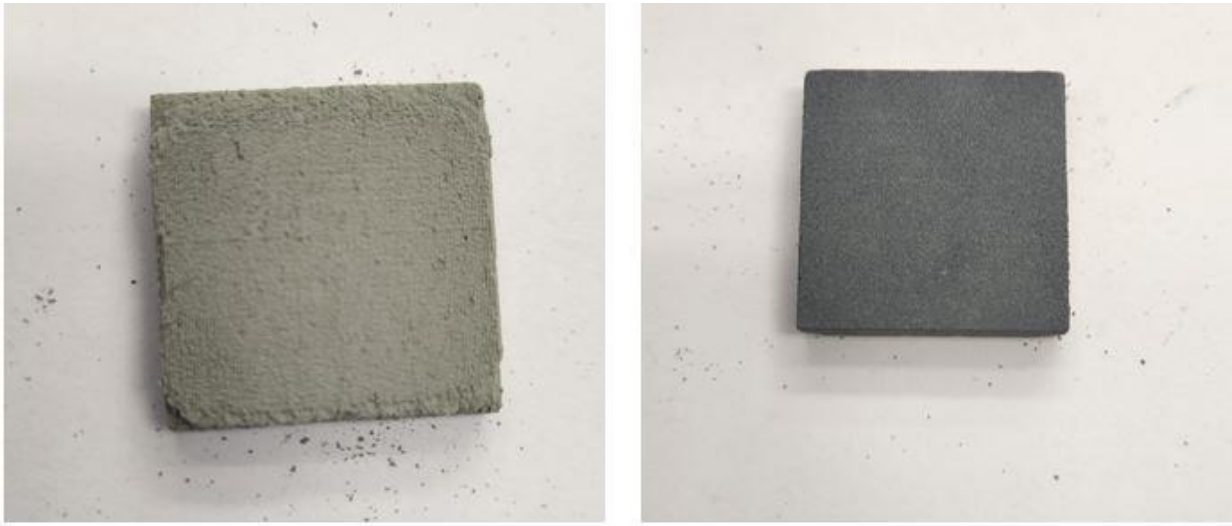

Figure 14. Cuboid printed with vendor-provided SiC (left) and Sigma Aldrich SiC (right).

These parts have not been densified and are in the green state. A Keyence VR-5000 Profilometer was used to get dimensional information for some of the cuboids to determine the tolerances of the X25Pro with initial settings. Figure 15, Figure 16, and

Table 1 summarize the measured dimensions and present their comparison with the CAD dimensions. Table 2 summarizes the average length and width for each powder, as well as the standard deviation for each dimension. Based on these results, the Sigma Aldrich SiC produces a more consistent part while being approximately 300 µm off from the CAD model. As

Table 1 and Table 2 show, both the length and width were generally off by approximately 300 µm compared to the CAD model for both powders; however, this could likely be improved via process setting optimization. For example, settings for the Innovent+ binder jet system were optimized to achieve a slight overprint of ~200 µm. The X25Pro can likely reach that threshold as well, with proper optimization.

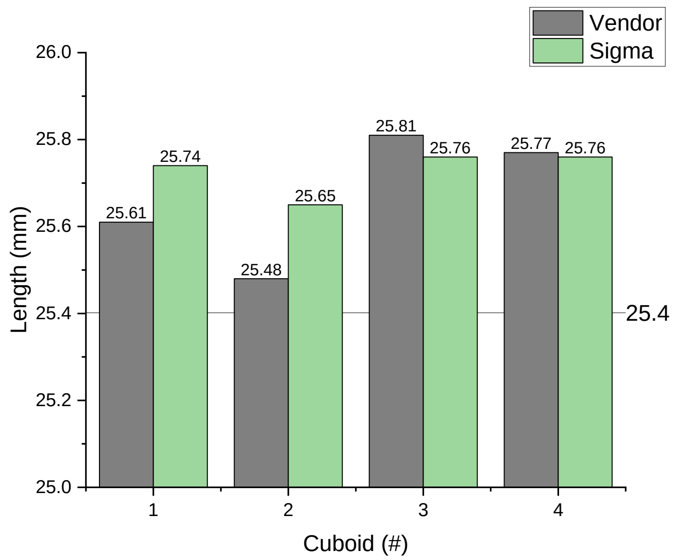

Figure 15: Bar graph showing deviation from CAD dimensions for both powders in the length.

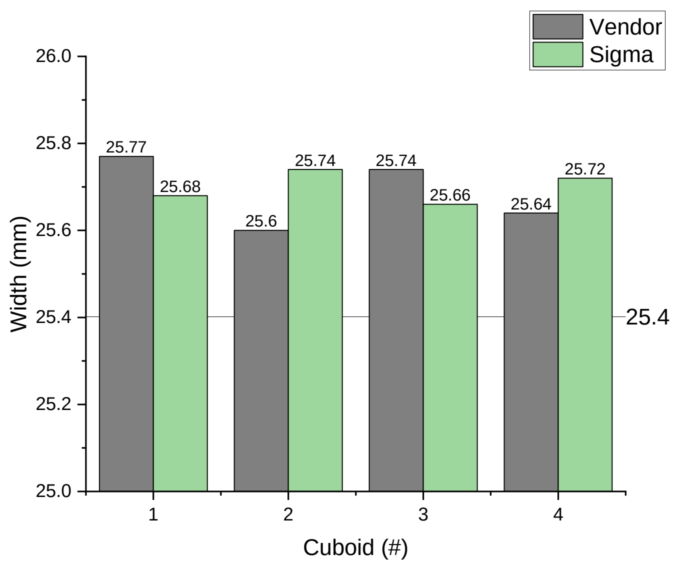

Figure 16: Bar graph showing deviation from CAD dimensions for both powders in the width.

Table 1. Keyence dimensional measurements of cuboids printed using vendor-supplied SiC powder and Sigma Aldrich SiC powder

Sample # (powder)	Length (mm)	Deviation from CAD (mm)	Width (mm)	Deviation from CAD (mm)
1 (Vendor)	25.61	0.21	25.77	0.37
1 (Sigma)	25.74	0.34	25.68	0.28
2 (Vendor)	25.48	0.08	25.60	0.20
2 (Sigma)	25.65	0.25	25.74	0.34
3 (Vendor)	25.81	0.41	25.74	0.34
3 (Sigma)	25.76	0.36	25.66	0.26
4 (Vendor)	25.77	0.37	25.64	0.24
4 (Sigma)	25.76	0.36	25.72	0.32

Table 2. Average length and width and standard deviation for each powder

Powder	Average length (mm)	Standard deviation (length)	Average width (mm)	Standard deviation (Width)
Vendor	25.67	0.152	25.69	0.081
Sigma	25.73	0.053	25.70	0.037

5. CONCLUSIONS AND FUTURE WORK

Newly scaled up infrastructure available at ORNL will enable new levels of ceramic manufacturing and combined with advanced monitoring technologies, this will be essential to support future digitally-informed certification of AM components. The X25Pro binder jet system is capable of printing large-scale SiC components with in-situ process monitoring. Peregrine has been incorporated into the X25Pro system, and a test print was performed to compare the vendor-supplied SiC powder with the typical SiC from Sigma Aldrich used for the TCR program. The Sigma Aldrich SiC powder appeared to perform much better, as it produced a smoother surface and flowed very well. The process settings currently result in dimensions that are ~300 µm larger than the nominal CAD dimensions, but this can likely be improved with further optimization similar to what was done previously under the TCR program with different binder jet systems.

Direct comparisons between prints with the same SiC feedstock will be made on the Innovent+ and the X25Pro systems to determine dimensional tolerances, surface roughness, and density differences between the two. Further optimization of the X25Pro will be a future focus as once job process settings have been optimized, larger parts will be printed and densified via the large-scale AVS CVI system. All these efforts will incorporate the Peregrine tool to produce digital data on the X25Pro to inform material certification. ORNL's lab space will be vital for supporting future needs from advanced reactor developers to deploy the next generation of passively-safe nuclear operations and will be available to support other AM SiC development under the DOE-NE AMMT program.

6. REFERENCES

1. Deck, C.P., et al., *Fabrication of SiC–SiC composites for fuel cladding in advanced reactor designs.* Progress in Nuclear Energy, 2012. **57**: p. 38-45.
2. Schleicher, R. *Advanced Reactors*. 9/1/2022]; Available from: https://ga.com/nuclear-fission/advanced-reactors.
3. Katoh, Y., et al., *Current status and recent research achievements in SiC/SiC composites.* Journal of Nuclear Materials, 2014. **455**(1): p. 387-397.
4. Terrani, K.A., et al., *Irradiation stability and thermo-mechanical properties of NITE-SiC irradiated to 10 dpa.* Journal of Nuclear Materials, 2018. **499**: p. 242-247.
5. Katoh, Y., et al., *Radiation effects in SiC for nuclear structural applications.* Current Opinion in Solid State and Materials Science, 2012. **16**(3): p. 143-152.
6. Katoh, Y., et al., *Continuous SiC fiber, CVI SiC matrix composites for nuclear applications: Properties and irradiation effects.* Journal of Nuclear Materials, 2014. **448**(1): p. 448-476.
7. Katoh, Y. and L.L. Snead, *Silicon carbide and its composites for nuclear applications – Historical overview*. Journal of Nuclear Materials, 2019. **526**: p. 151849.
8. Byun, T.S., et al., *Mechanical and Thermophysical Properties of 3D-Printed SiC before and after Neutron Irradiation – FY 2021*. 2021: United States.
9. Ade, B.J., et al., *Candidate Core Designs for the Transformational Challenge Reactor.* Journal of Nuclear Engineering, 2021. **2**(1): p. 74-85.
10. Betzler, B.R., et al., *Conceptual Design of the Transformational Challenge Reactor.* Nuclear Science and Engineering, 2022: p. 1-26.
11. Betzler, B.R., et al., *Transformational Challenge Reactor preconceptual core design studies.* Nuclear Engineering and Design, 2020. **367**: p. 110781.
12. Kile, R.F., et al., *Transformational challenge reactor analysis to inform preconceptual core design decisions: Sensitivity study of transient analysis in a hydride-moderated microreactor.* Nuclear Engineering and Design, 2021. **376**: p. 111122.
13. See, N.D., S. Cetiner, and B.R. Betzler, *Design Optimization of the Transformational Challenge Reactor Outlet Plenum.* Nuclear Science and Engineering, 2022: p. 1-20.
14. Sobes, V., et al., *AI-based design of a nuclear reactor core.* Scientific Reports, 2021. **11**(1): p. 19646.
15. Talamo, A., et al., *Multiphysics Analyses of the Bottom Components of the 3D Printed Transformational Challenge Reactor.* Nuclear Technology, 2022. **208**(9): p. 1433-1452.
16. Hu, X., et al., *Handbook on the Material Properties of Yttrium Hydride for High Temperature Moderator Applications*. 2021: United States.
17. Hu, X., et al., *Fabrication of yttrium hydride for high-temperature moderator application.* Journal of Nuclear Materials, 2020. **539**: p. 152335.
18. Trofimov, A.A., et al., *Thermophysical properties and reversible phase transitions in yttrium hydride.* Journal of Nuclear Materials, 2020. **542**: p. 152569.
19. Kane, K., et al., *Air oxidation of yttrium hydride as a high temperature moderator for thermal neutron spectrum fission reactors.* Journal of Nuclear Materials, 2021. **556**: p. 153166.
20. Chapman, C.W., et al., *Thermal neutron scattering measurements and modeling of yttrium-hydrides for high temperature moderator applications.* Annals of Nuclear Energy, 2021. **157**: p. 108224.
21. Hu, X. and K.A. Terrani, *Thermomechanical properties and microstructures of yttrium hydride.* Journal of Alloys and Compounds, 2021. **867**: p. 158992.
22. Ade, B.J., et al., *Reactor Physics Considerations for Use of Yttrium Hydride Moderator.* Nuclear Science and Engineering, 2022: p. 1-20.
23. Li, M., et al., *Creep behavior of 316 L stainless steel manufactured by laser powder bed fusion.* Journal of Nuclear Materials, 2021. **548**: p. 152847.

24. Terrani, K., B. Jolly, and M. Trammell, *3D printing of high-purity silicon carbide.* Journal of the American Ceramic Society, 2020. **103**(3): p. 1575-1581.
25. Koyanagi, T., et al., *Additive manufacturing of silicon carbide for nuclear applications.* Journal of Nuclear Materials, 2021. **543**: p. 152577.
26. Terrani, K.A., B.C. Jolly, and J.M. Harp, *Uranium nitride tristructural-isotropic fuel particle.* Journal of Nuclear Materials, 2020. **531**: p. 152034.
27. Terrani, K.A., et al., *Architecture and properties of TCR fuel form.* Journal of Nuclear Materials, 2021. **547**: p. 152781.
28. Scime, L., A. Singh, and V. Paquit, *A scalable digital platform for the use of digital twins in additive manufacturing.* Manufacturing Letters, 2022. **31**: p. 28-32.
29. Scime, L., et al., *Layer-wise anomaly detection and classification for powder bed additive manufacturing processes: A machine-agnostic algorithm for real-time pixel-wise semantic segmentation.* Additive Manufacturing, 2020. **36**: p. 101453.
30. Huning, A.J., W.M. Kirkland, and K.A. Terrani, *Transformational Challenge Reactor Safety Design and Radionuclide Retention Strategy.* Nuclear Science and Engineering, 2021: p. 1-17.
31. Sweeney, D.C., A.M. Schrell, and C.M. Petrie, *An Adaptive Reference Scheme to Extend the Functional Range of Optical Backscatter Reflectometry in Extreme Environments.* IEEE Sensors Journal, 2021. **21**(1): p. 498-509.
32. Sweeney, D.C. and C.M. Petrie, *Expanding the range of the resolvable strain from distributed fiber optic sensors using a local adaptive reference approach.* Optics Letters, 2022. **47**(2): p. 269-272.
33. Petrie, C.M., et al., *Embedded sensors in additively manufactured silicon carbide.* Journal of Nuclear Materials, 2021. **552**: p. 153012.
34. Sweeney, D.C., D.M. Sweeney, and C.M. Petrie, *Graphical Optimization of Spectral Shift Reconstructions for Optical Backscatter Reflectometry.* Sensors, 2021. **21**(18).
35. Cetiner, S. and P. Ramuhalli, *Transformational Challenge Reactor Autonomous Control System Framework and Key Enabling Technologies*. 2019: United States.
36. Ramuhalli, P. and S.M. Cetiner, *Concepts for Autonomous Operation of Microreactors*. 2019: United States.
37. Terrani, K.A., et al., *Irradiation stability and thermomechanical properties of 3D-printed SiC.* Journal of Nuclear Materials, 2021. **551**: p. 152980.
38. Lach, T.G., et al., *Characterization of radiation damage in 3D printed SiC.* Journal of Nuclear Materials, 2022. **559**: p. 153459.
39. Byun, T.S., et al., *Mechanical behavior of additively manufactured and wrought 316L stainless steels before and after neutron irradiation.* Journal of Nuclear Materials, 2021. **548**: p. 152849.
40. Woolstenhulme, N., et al., *TREAT Testing of Additively Manufactured SiC Canisters Loaded with High Density TRISO Fuel for the Transformational Challenge Reactor Project.* J. Nucl. Mater.
41. *Ultra Safe Nuclear licenses ORNL method to 3D print advanced reactor components*. 2022 [cited 2022 8/18/2022]; Available from: https://www.ornl.gov/news/ultra-safe-nuclear-licenses-ornl-method-3d-print-advanced-reactor-components.
42. *BWXT to Lead $106.6 Milion Microreactor Design Project*. 2020 [cited 2022 8/18/2022]; Available from: https://www.bwxt.com/news/2020/12/23/BWXT-to-Lead-1066-Million-Microreactor-Design-Project.
43. Trammell, M.P., et al., *Advanced Nuclear Fuel Fabrication: Particle Fuel Concept for TCR.* 2019.